

**SUSITNA  
HYDROELECTRIC PROJECT**

FEDERAL ENERGY REGULATORY COMMISSION  
PROJECT No. 7114

**RESPONSE OF PHOTOSYNTHETICALLY  
ACTIVE RADIATION AT THE EUPHOTIC  
SURFACE TO ALTERED TURBIDITY  
AND STREAMFLOW REGIMES OF  
THE MIDDLE SUSITNA RIVER**

PREPARED BY



**Trihey &  
Associates**  
Aquatic Resource  
Specialists

UNDER CONTRACT TO

**HARZA-EBASCO**  
SUSITNA JOINT VENTURE

**DRAFT REPORT**

**DECEMBER 1985**  
DOCUMENT No. 2971

***Alaska Power Authority***

SUSITNA HYDROELECTRIC PROJECT

RESPONSE OF PHOTOSYNTHETICALLY ACTIVE RADIATION  
AT THE EUPHOTIC SURFACE TO ALTERED TURBIDITY AND  
STREAMFLOW REGIMES OF THE MIDDLE SUSITNA RIVER

Report by  
Trihey and Associates  
Gregory S. Reub  
Robert C. Wilkinson  
Robert G. Elder

Under Contract to  
Harza-Ebasco Susitna Joint Venture

Prepared for  
Alaska Power Authority

Draft Report  
December 20, 1985

**NOTICE**

**ANY QUESTIONS OR COMMENTS CONCERNING  
THIS REPORT SHOULD BE DIRECTED TO  
THE ALASKA POWER AUTHORITY  
SUSITNA PROJECT OFFICE**

TABLE OF CONTENTS

	<u>PAGE</u>
INTRODUCTION.....	1
METHODS.....	6
RESPONSE OF EUPHOTIC SURFACE AREA TO CHANGES IN DISCHARGE AND TURBIDITY.....	17
SITE-SPECIFIC RESPONSE OF LIGHT ENERGY AVAILABLE TO THE EUPHOTIC SURFACE AREA.....	20
SUMMARY.....	40
REFERENCES.....	43

## INTRODUCTION

Primary productivity is important to the production of food organisms for juvenile salmonids. Primary productivity in streams and rivers is dependent on the ability of sunlight to reach the streambed in sufficient amounts to support photosynthesis. Algal production is related to the intensity of light as well as depth of penetration (Hynes 1979). Factors affecting light penetration to streambed surfaces will also affect primary productivity (Lloyd 1985). Two important factors that influence the amount of light reaching the streambed are depth, as regulated by streamflow, and turbidity. It follows, therefore, that determining the effects of streamflow and turbidity on light penetration can be used to estimate their effects on primary production.

The euphotic zone is defined as that portion of the submerged streambed where light intensity is greater than one percent of the light intensity at the water surface. The lower limit of this zone is termed the compensation depth. The significance of the compensation depth is that it approximates the point where energy fixation by algal photosynthesis is equal to the organisms' own respiratory requirements (Moss 1980). Thus, compensation depth can be used as the lower boundary in the relationship between turbidity and depth of light penetration. The limit of photosynthetically effective penetration must be defined through field measurements of light attenuation.

This paper presents preliminary results from a simulation model that was developed to forecast the response of photosynthetically active radiation (PAR) at the euphotic zone to changes in mainstem discharge and turbidity. The model was applied at eight study sites located in the middle Susitna River. Results from site-specific and time series analyses are used to refine the euphotic surface area response model introduced in April 1985 (Reub et al. 1985). One purpose of this technical memo is to demonstrate the utility of the model for evaluating the influence of altered streamflows and turbidities on primary production in the middle Susitna River. Another purpose is to provide an initial forecast of changes in the amount of light energy available for photosynthesis on a seasonal basis as a result of project construction and operation.

The euphotic surface area response model estimates the amount of PAR that reaches the euphotic surface area at a certain time. This is accomplished by determining the amount of PAR that reaches the submerged streambed at a certain depth within the compensation depth and multiplying that amount of energy times the surface area found at that depth. This gives the total energy received at depth, which is then summed for all depths down to the compensation depth. This summation represents the total amount of PAR available for an entire site. The model can be expressed in mathematical terms by the following basic equation:

$$E_t = \sum_{Z=0}^{Z_c} (I_z \times A_z)$$

where  $E_t$  = Gross Rate of Energy Input to Euphotic Surface Area at Time in einsteins

$I_z$  = Areal Rate of Energy Input to Surface Area at Depth z (einsteins/sq ft)

$A_z$  = Surface Area at Depth z (ft<sup>2</sup>)

The steps necessary to numerically define the parameters in the above equation are shown in Figure 1. Solar insolation, turbidity regimes and mainstem discharge (boxes on left of flow diagram) vary on a seasonal basis and are considered the "driving variables" in this model. Solar insolation, or the light available at the water surface, and turbidity determine the amount of light that is extinguished as it passes through the water column. Mainstem discharge determines the depth of water and the amount of wetted surface area within a site.

The euphotic surface area response model uses stream cross section and stage-discharge data (IFG<sup>1</sup> hydraulic models) to apportion the entire wetted surface area of a study site into incremental depths as a function of discharge. Compensation depth, influenced by turbidity, is used to define which depths are within the euphotic zone. This model then forecasts streamflow and turbidity-dependent response curves for the amount of PAR transmitted through the water column. The model does not forecast actual photosynthetic rates. It is assumed that primary

<sup>1</sup> Instream Flow Group, now known as Instream Flow and Aquatic Systems Group (Milhouse et al. 1984).

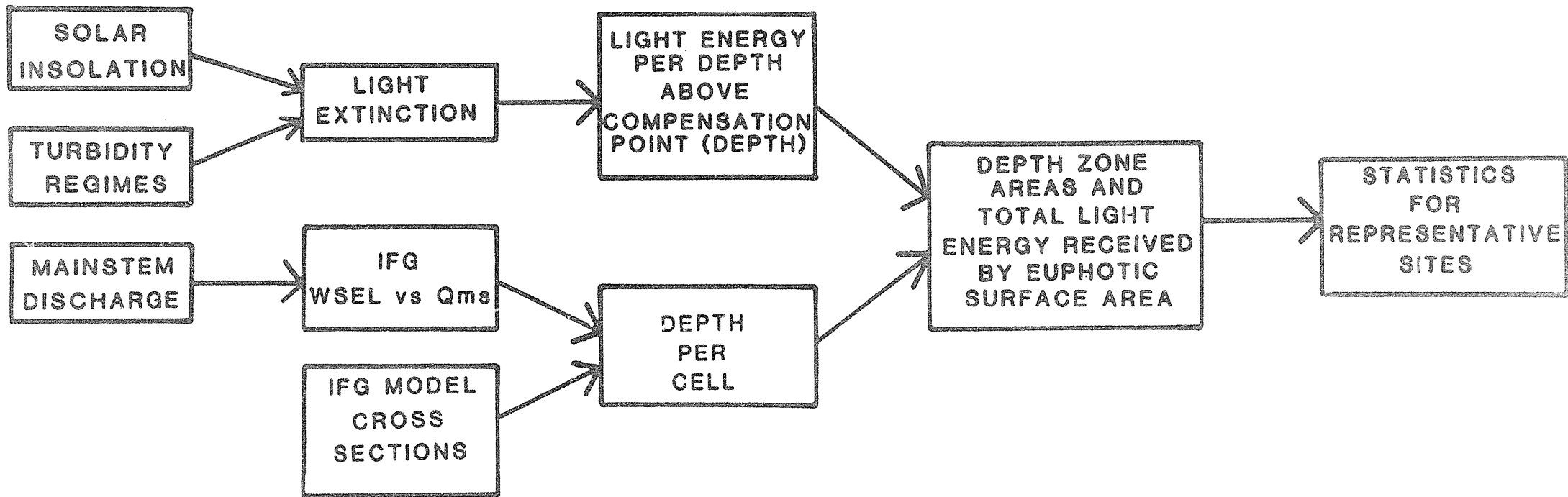


Figure 1. A flow diagram of the basic components used in the euphotic surface area response model.

production only occurs on the submerged streambed between the water's edge and a point bounded by the compensation depth. Because this model is intended for riverine application, primary production is not assumed to occur within the water column as it would were lakes or estuaries being evaluated. The following methods section provides analytical descriptions of the model components and presents actual input data used in the model.

## METHODS

### Determination of Solar Insolation

The amount of PAR available to the surface of the water depends on the latitude of the river basin, time of year, basin topography, and prevailing meteorological conditions. Only a few studies have measured solar radiation inputs in southcentral Alaska. Coffin (1984) collected two years of solar radiation data at various locations near the Susitna River, and Branton et al. (1972) collected 11 years of solar radiation data at Palmer, Alaska. This analysis uses solar radiation data collected over a two-year period at Big Lake, Alaska by Rowe (1985). The Big Lake data provide PAR values at the lake surface throughout the year (Table 1).

Table 1. Estimated mean monthly photosynthetically active radiation (PAR) in einsteins per square foot.

MONTH	AVERAGE PAR <sup>1</sup>	MONTH	AVERAGE PAR <sup>1</sup>
JANUARY	4	JULY	91
FEBRUARY	17	AUGUST	74
MARCH	92	SEPTEMBER	46
APRIL	66	OCTOBER	20
MAY	100	NOVEMBER	5
JUNE	114	DECEMBER	2

<sup>1</sup> Estimated for 1984 and 1985 at Big Lake, Alaska

Source: Timothy G. Rowe (1985)

## METHODS

### Determination of Solar Insolation

The amount of PAR available to the surface of the water depends on the latitude of the river basin, time of year, basin topography, and prevailing meteorological conditions. Only a few studies have measured solar radiation inputs in southcentral Alaska. Coffin (1984) collected two years of solar radiation data at various locations near the Susitna River, and Branton et al. (1972) collected 11 years of solar radiation data at Palmer, Alaska. This analysis uses solar radiation data collected over a two-year period at Big Lake, Alaska by Rowe (1985). The Big Lake data provide PAR values at the lake surface throughout the year (Table 1).

Table 1. Estimated mean monthly photosynthetically active radiation (PAR) in einsteins per square foot.

MONTH	AVERAGE PAR <sup>1</sup>	MONTH	AVERAGE PAR <sup>1</sup>
JANUARY	4	JULY	91
FEBRUARY	17	AUGUST	74
MARCH	92	SEPTEMBER	46
APRIL	66	OCTOBER	20
MAY	100	NOVEMBER	5
JUNE	114	DECEMBER	2

<sup>1</sup> Estimated for 1984 and 1985 at Big Lake, Alaska

Source: Timothy G. Rowe (1985)

## Determination of Turbidity Regimes

Middle Susitna River turbidity levels under natural conditions at Gold Creek range from 1 to 1,000 NTU (nephelometric turbidity units) with average summer turbidities of approximately 200 NTU and with winter turbidities of less than 5 NTU (Trihey and Associates et al. 1985). With-project turbidity levels are expected to be less variable during the year with increases over natural turbidities expected in the winter and decreases expected during the summer months.

Several project documents were reviewed to arrive at a natural turbidity regime that represents monthly values for the entire season (Acres American Inc. 1982; Alaska Department of Fish and Game 1982, 1983a, 1983b; Alaska Power Authority 1985). Figure 2 illustrates the estimated natural turbidity values used in the time series analysis. These values are derived by drawing a smooth curve through data points collected during the 1983 open water season at Gold Creek Camp, River Mile (RM) 136.8, and the Talkeetna Fishwheel, RM 103.0 (Estes et al. 1984).

Estimates of with-project turbidity regimes were determined by Harza-Ebasco Susitna Joint Venture (Alaska Power Authority 1985). Their analysis uses an NTU/TSS (total suspended sediment) ratio of 2:1 to forecast turbidities for with-project conditions (Table 2). Several studies identify the relationship between TSS and turbidity. Typical relationships developed in Alaskan lentic (lake) environments associated with glaciated drainages include those at Eklutna Lake (R & M Consultants 1982), Bradley Lake (Ott Water Engineers Inc. 1981) and Tustumena Lake (Scott 1982). These studies suggest NTU/TSS ratios of

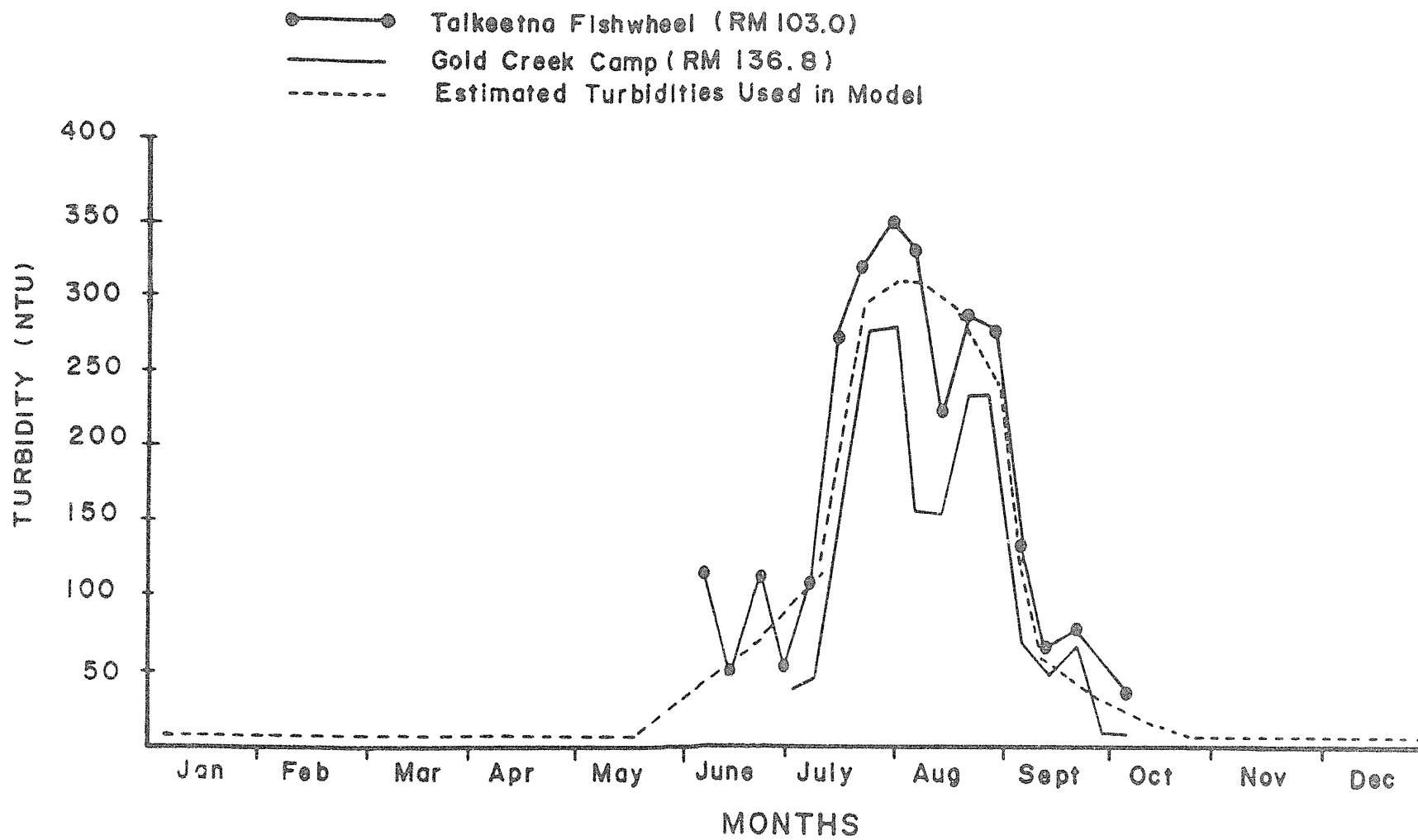


Figure 2. Actual turbidity values at Talkeetna Fishwheel (RM 103.0) and Gold Creek Camp (RM 36.8) with estimated turbidities used in this model.

approximately 2:1 or greater. This conversion factor results in a minimal turbidity estimate (Alaska Power Authority 1985), although it is recognized that the actual ratio of NTU/TSS may vary considerably as evidenced by the range of values discussed in the above references.

For the purposes of our analysis only two operational scenarios, Stage I and Stage III, were evaluated to illustrate the range of with-project conditions that are expected to occur.

Table 2. Estimated monthly average turbidities (NTU) for natural and with-project scenarios.

MONTH	TURBIDITIES		
	NATURAL <sup>1</sup>	STAGE I <sup>2</sup> NTU/TSS RATIO 2:1	STAGE III <sup>2</sup> NTU/TSS RATIO 2:1
JANUARY	3	130	110
FEBRUARY	3	110	100
MARCH	3	86	50
APRIL	3	60	50
MAY	32	70	34
JUNE	119	170	70
JULY	306	260	150
AUGUST	149	220	150
SEPTEMBER	24	180	110
OCTOBER	6	200	100
NOVEMBER	3	190	140
DECEMBER	3	166	136

<sup>1</sup> Estimated from data collected during the open water season (Estes et al. 1984).

<sup>2</sup> Estimated by converting TSS projections to NTU units (Alaska Power Authority 1985).

### Determination of Compensation Depth and Rate of Light Extinction

Since the rate of light extinction and compensation depth must be calculated over the range of turbidity levels analyzed, a relationship between light extinction ( $k$ ) and turbidity was generated using Susitna-specific data collected during August and September 1985. Total vertical light extinction coefficient measurements were made using the methodology described by Van Nieuwenhyse (1983). Twenty measurements of compensation depth were made near the confluence of the Susitna, Chulitna and Talkeetna rivers under turbidities ranging from 5 to 179 NTU. Light extinction coefficients were plotted against turbidity and the relationship was described by linear regression analysis (Figure 3).

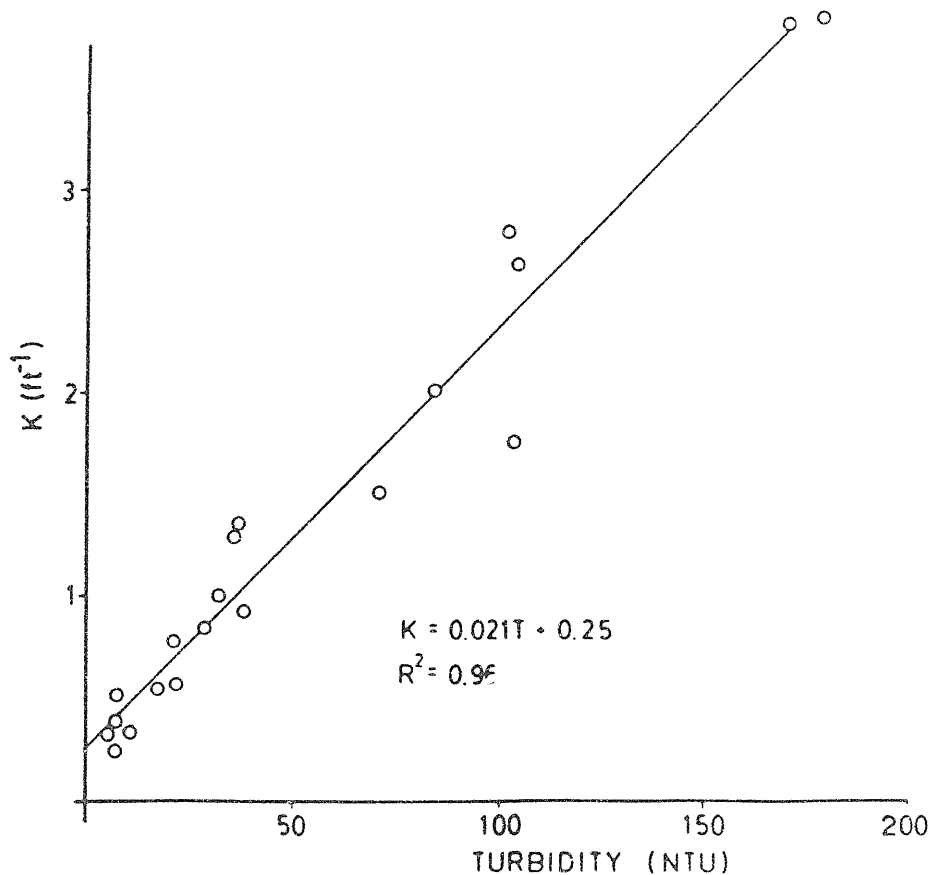


Figure 3. Linear regression of Susitna-specific light extinction coefficients versus turbidity.

The relationship between compensation depth and turbidity for the Susitna River is described by the equation  $Z_c = 4.61/0.021(NTU)+0.25$  (Figure 4). This equation was formulated by incorporating the regression equation presented in Figure 3 into the derivation described by Van Nieuwenhuyse (1984).

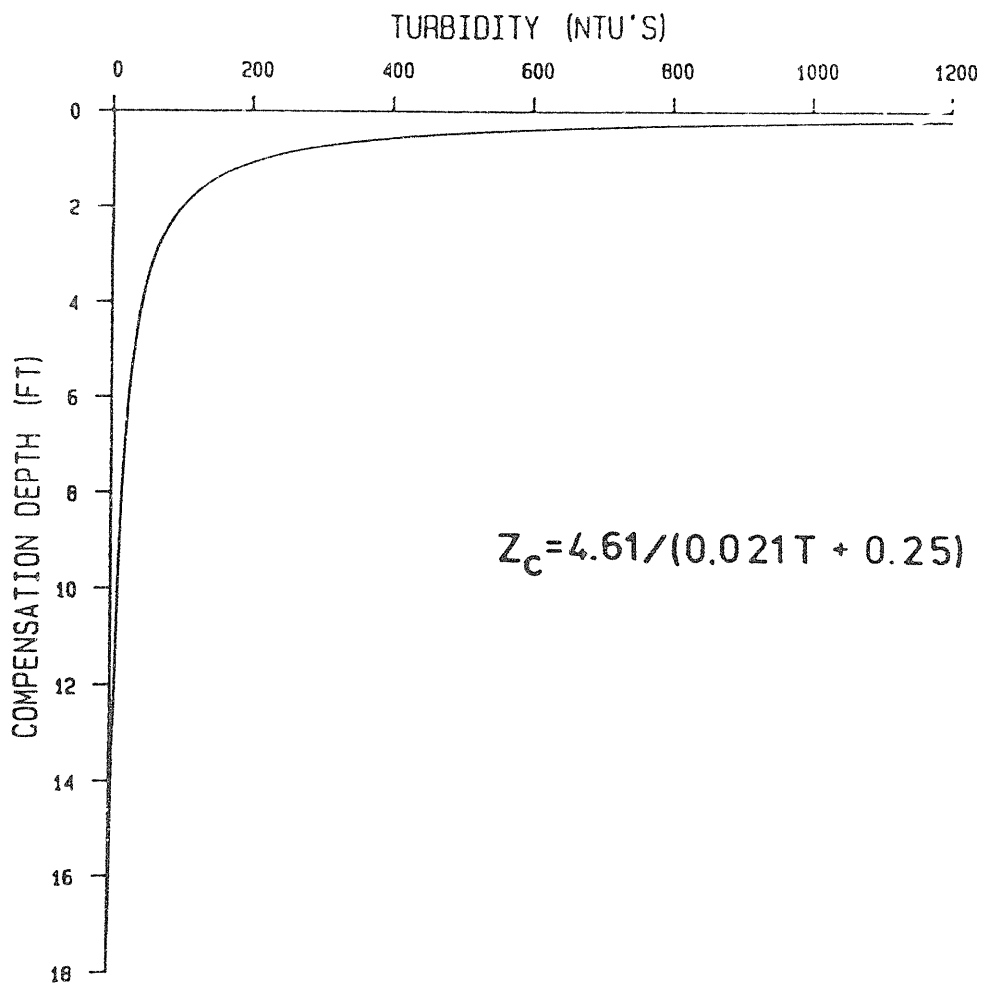


Figure 4. Relationship between turbidity and compensation depth for the Susitna River.

## Determination of Mainstem Discharge

Mean monthly streamflows were used in this analysis. Average weekly mainstem flows for both natural and with-project conditions were developed by the Harza Ebasco Susitna Joint Venture based on 34 years of record at Gold Creek (Alaska Power Authority 1985). These flows were averaged to obtain the monthly values in Table 3. Only streamflows for Stage I and Stage III operation scenarios were used to evaluate with-project conditions.

Table 3. Estimated mean monthly flows (cfs) for natural and with-project scenarios.

MONTH	STREAMFLOW		
	NATURAL	STAGE I	STAGE III <sup>1</sup>
JANUARY	1,543	8,135	8,256
FEBRUARY	1,317	7,591	8,112
MARCH	1,169	5,732	7,280
APRIL	1,441	4,108	6,623
MAY	13,483	6,380	7,643
JUNE	27,795	13,324	9,223
JULY	24,390	14,492	13,156
AUGUST	21,911	18,276	18,489
SEPTEMBER	13,493	14,230	13,406
OCTOBER	5,825	7,903	7,720
NOVEMBER	2,589	7,800	8,244
DECEMBER	1,844	9,120	9,011

Source: Alaska Power Authority (1985).

<sup>1</sup> These values represent an estimated early Stage III flow scenario.

## Determination of Site Geometry

Stream channel geometry influences the response of the euphotic surface area to changes in discharge (water surface elevation) and turbidity. Site geometry was determined using the IFG cross sections surveyed for the middle Susitna River modeling studies. These cross sections were used to describe the lateral distribution of streambed elevations.

Cell depth was determined using the water surface elevation (WSEL) corresponding to a given discharge and the streambed elevations along the surveyed cross section. The WSEL's used in this analysis were forecast using hydraulic models and associated rating curve equations (Estes et al. 1984, and Hilliard et al. 1985). A relationship between WSEL and discharge was established for each transect.

The maximum resolution of the depth calculations is a function of the cell size. Point measurements of depth more accurately approximate the average depth of the cells as cell size is reduced. Depths associated with one-foot cell widths were necessary for good resolution at high turbidities (small increments of depth). This cell resolution was achieved by linear interpolation between surveyed streambed elevations on the cross sections.

The reach length represented by a particular cross section was determined from inspection of aerial photography, longitudinal streambed profiles and field notes. In those instances where right and left streambank distances between adjacent cross sections differed, reach lengths for individual cells were determined by linear interpolation

using the right and left bank distances. Cell surface area is the area of the rectangle defined by width multiplied by mean reach length.

#### Calculation of Light Energy Available to Euphotic Surface Area

The total light energy available to the euphotic surface area is calculated in three steps. First, the compensation depth is defined as a function of turbidity. For each cell possessing a depth equal to or less than the compensation depth, the cell area is calculated. The sum of these areas defines the euphotic surface area. The model uses the decay function describing light attenuation with depth to determine the amount of light energy reaching the streambed within each cell. The total light energy reaching the euphotic surface is calculated by summing the light energies at the streambed surface for all the cells. These calculations are repeated for each combination of flow and turbidity being evaluated.

#### Site Selection

Stream channel geometry influences the response of euphotic surface area to changes in discharge and turbidity. It is therefore important that cross sectional data used in the model represent typical middle Susitna River habitat types that are expected to be affected by altered discharge and turbidity levels.

Six major habitat types have been identified in the middle Susitna River (ADF&G 1983a). Tributary, tributary mouth, and upland slough habitats are normally clear and not expected to become turbid as a result of the construction and operation of the proposed Susitna hydroelectric project. However, the natural turbidity regimes within mainstem, side channel, and side slough habitats are expected to be altered. A three-step process was used to select eight model sites that represent mainstem, side channel, and side slough habitats. Initially, project hydrologists and biologists were consulted. Aerial photography was reviewed to provide a quick assessment of the response of wetted surface area to mainstem discharge at various sites and to identify whether these sites might transform from turbid to clearwater areas as mainstem discharge declines. Hydraulic and morphologic attributes identified by Aaserude et al. (1985) to classify sites into representative groups were used as indicators of "representativeness".

Table 4 describes the hydrologic and morphologic characteristics of the 10 representative groups developed by Aaserude et al. (1985). Also shown to the right of the definitions are the model sites chosen for this analysis. Representative groups with similar channel geometry and morphologic attributes are represented by the same model or combination of models (i.e., groups III and VIII, V and VI, IX and X). However, model results have not been extrapolated to the middle Susitna River in proportion to the surface areas of the various representative groups. Upland sloughs (Group I) are not expected to be affected by the project and thus are not included in the analysis.

Table 4. Primary hydrologic, hydraulic and morphologic characteristics of representative groups identified for the middle Susitna River.

REPRESENTATIVE GROUP	DESCRIPTION	MODELING SITE
I	Predominantly upland sloughs. The specific areas comprising this group are highly stable due to the persistence of non-breached conditions (i.e., possess high breaching flows). Specific area hydraulics are characterized by pooled clear water with velocities frequently near 0.0 fps and depths greater than 1.0 ft. Pools are commonly connected by short riffles where velocities are less than 1.0 fps and depths are less than 0.5 ft.	No Project Affect
II	This group includes specific areas commonly referred to as side sloughs. These sites are characterized by relatively high breaching flows (>19,500 cfs), clear water caused by upwelling groundwater, and large channel length-to-width ratios (>15:1).	126.0R
III	Intermediate breaching flows and relatively broad channel sections typify the specific areas within this representative group. These sites are side channels which transform into side sloughs at Mainstem discharges ranging from 8,200 to 16,000 cfs. Lower breaching flows and smaller length to width ratios distinguish these sites from those in Group II. Upwelling groundwater is present.	128.8R
IV	Specific areas in this group are side channels that are breached at low discharges and possess intermediate mean reach velocities (2.0 to 5.0 fps) at a mainstem discharge of approximately 10,000 cfs.	112.6L 131.7L
V	This group includes mainstem and side channel shoal areas which transform to clear water side sloughs as mainstem flows recede. Transformations generally occur at moderate to high breaching discharges.	136.3R (From VI)
VI	This group is similar to the preceding one in that the habitat character of the specific areas is dominated by channel morphology. These sites are primarily overflow channels that parallel the adjacent mainstem, usually separated by a sparsely vegetated gravel bar. Upwelling groundwater may or may not be present. Habitat transformations within this group are variable both in type and timing of occurrence.	136.3R
VII	These specific areas are typically side channels which breach at variable yet fairly low mainstem discharges and exhibit a characteristic riffle/pool sequence. Pools are frequently large backwater areas near the mouth of the sites.	119.2R
VIII	The specific areas in this group tend to dewater at relatively high mainstem discharges. The direction of flow at the head of these channels tends to deviate sharply (>30 degrees) from the adjacent mainstem. Modeling sites from Groups II and III possessing representative post-breaching hydraulic characteristics are used to model these specific areas.	128.8R (From III)
IX	This group consists of mainstem and side channels, including indistinct (i.e., shoal) areas, characterized by low breaching discharges. Specific areas tend to either retain their habitat type character or transform from indistinct to distinct channels.	147.1L 101.5L
X	Large mainstem shoals and the margins of mainstem channels which show signs of upwelling are included in this representative group.	147.1L 101.5L (From IX)

Source: Aaserude et al. 1985

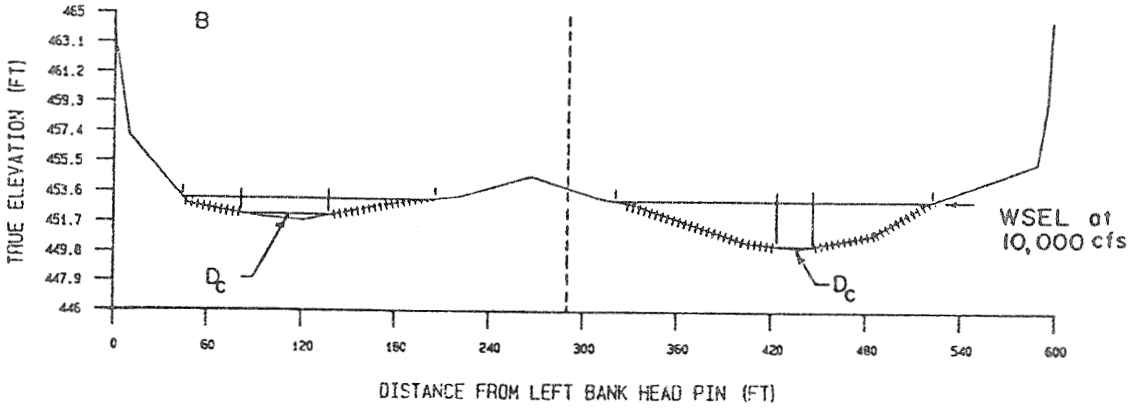
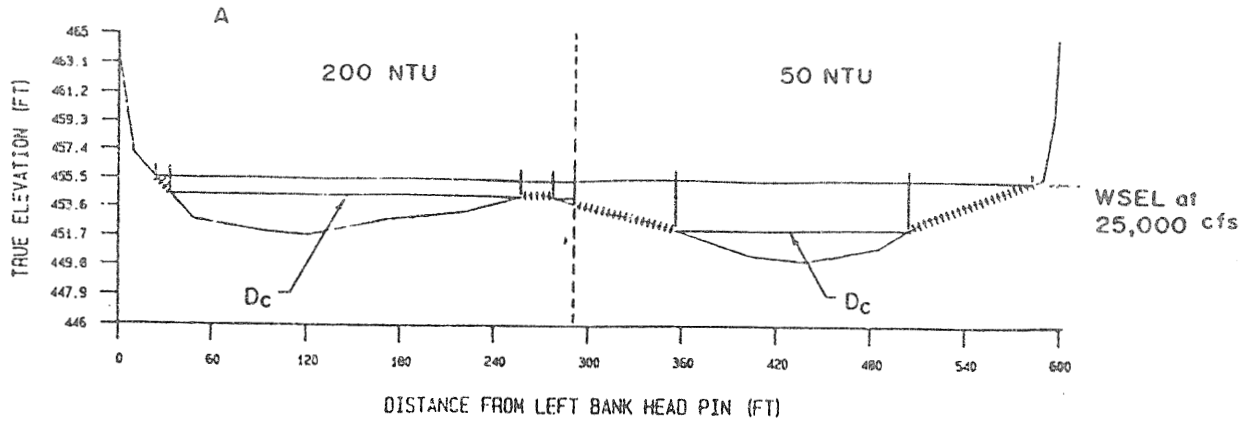
## RESPONSE OF EUPHOTIC SURFACE AREA TO CHANGES IN DISCHARGE AND TURBIDITY

An illustrative example of euphotic surface area response to variations in turbidity and flow is presented as Figure 5. Two types of channel geometry are used to demonstrate how the euphotic surface area responds to changes in water surface elevation (depth) and to turbidity (compensation depth). The top two illustrations are of a typical streambed cross section (transect 3) at Side Channel 6A at two stream flows. Water surface elevation for the same stream flows are shown for a typical cross section at Fat Canoe Island (Transect 5) in the bottom two illustrations. Each illustration is divided in half and the right and left portions of the illustration are assigned different turbidity values. Compensation depths corresponding to these turbidity values are indicated, and the width of the euphotic surface area (shown by cross hatching) is approximated by the width of the overlying water surface.

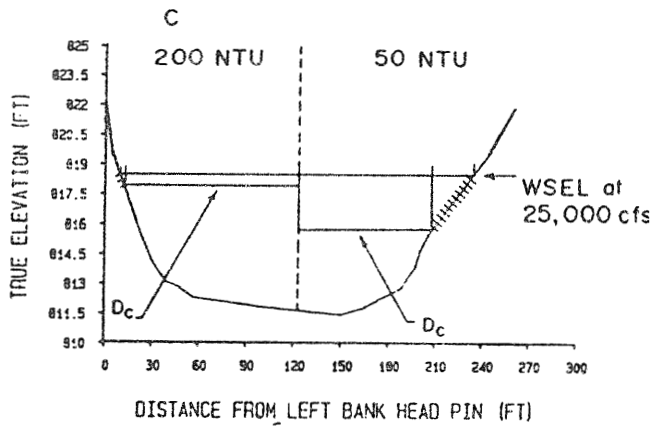
Side Channel 6A, representing broad shallow side channels, has a maximum depth of about 3.2 feet at 10,000 cfs and 5.6 feet at 25,000 cfs. In contrast, sites such as Fat Canoe Island with a well-incised, steep-sided channel have less variation in streambed elevations. Compensation depths for the turbidity levels used in this illustration are 3.5 feet for 50 NTU and 1.0 foot for 200 NTU.

In comparatively broad and shallow channels such as the Side Channel 6A site, relatively small changes in turbidity or flow can have a dramatic effect on the size of the euphotic surface area. When the flow drops from 25,000 cfs to 10,000 cfs at 50 NTU, the width of the euphotic surface area increases 48 percent in this example. Similarly, at stream

SIDE CHANNEL 6A - TRANSECT 3



FAT CANOE - TRANSECT FIVE



LEGEND	
	EUPHOTIC SURFACE AREA
Dc	COMPENSATION DEPTH
WSEL	WATER SURFACE ELEVATION

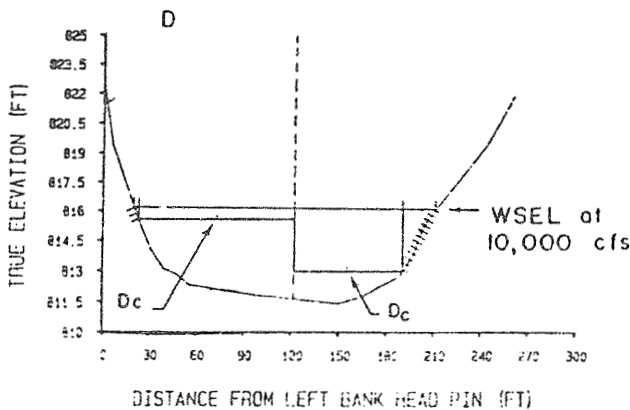


Figure 5. Hypothetical illustration of the effects of turbidity, discharge, and channel geometry on euphotic surface area response.

flows near 10,000 cfs a change in turbidity from 200 to 50 NTU results in a 75 percent increase in the euphotic surface area. This sensitivity to turbidity and stream flow is due to relatively broad, shallow areas (riffles, shoals and channel bottoms) being found at this site.

By reducing stream flow from 25,000 to 10,000 cfs at 50 NTU at the Fat Canon Island site, approximately a 10 percent change in the width of the euphotic surface area is observed. At stream flows near 10,000 cfs, a change in turbidity from 200 to 50 NTU increases the width euphotic surface area by 328 percent. This sensitivity to turbidity but insensitivity to streamflow is attributable to the steep gradient shorelines and incised nature of the cross sectional geometry.

## SITE-SPECIFIC RESPONSE OF LIGHT ENERGY AVAILABLE TO THE EUPHOTIC SURFACE AREA

Because of the influence of channel geometry on euphotic surface area, the model was applied at eight locations on the middle Susitna River. Application of the model at each site is discussed separately. First, site characteristics that influence the euphotic surface area response are described. Next, a family of light energy response curves is presented for six turbidity values from 10 to 800 NTU and a range of mainstem discharges between 5,000 and 35,000 cfs. A PAR value of 50 einsteins per square foot was used to determine the family of response curves for each site. Finally, annual response curves are presented for the site using seasonal solar insolation, turbidities and streamflows for both natural and two with-project scenarios. The seasonal values for each variable used in the time series analysis are presented in the methods section.

The time series analysis curves for natural conditions include only the open water season (May through October). With-project curves are presented for the entire year; however, they do not incorporate any effects of ice and snow cover. For this reason, the discussion of anticipated project effects on available light energy at the euphotic surface is generally limited to the open water season.

Several factors suggest that light intensity beneath an ice and snow cover is not biologically significant at this latitude. Two important factors are the seasonal reduction in PAR during the winter months and the reflective effect of the snow and ice cover on incoming light. Rowe

(1985) compared the hourly PAR at Big Lake, Alaska for the summer solstice (June 21) and winter solstice (December 21). At summer solstice, the lake received 55.8 Einsteins per square meter during the 20 hours of daylight, whereas the six hours of daylight at the winter solstice provided only 0.9 Einsteins per square meter. Rowe also found a major difference between reflection coefficients between summer and winter. During summer about five to ten percent of the solar radiation was reflected, but in the winter from 85 to 95 percent was reflected. These results agree with studies on reflection by Roulet and Adams (1984) and Chow, ed. (1964).

#### Fat Canoe Island (RM 147.1L)

Fat Canoe represents typical mainstem habitat. This site and the following site (Whiskers West) are associated with Representative Groups IX and X (refer to Table 4). The channel at Fat Canoe is approximately 820 feet wide throughout its length. The entire left bank is near vertical; the right bank has a steep to moderate gradient. An exposed cobble shoreline extends the full length of the right bank (approximately 2,070 feet). The breaching flow for this site is less than 5,000 cfs. Therefore, it conveys turbid mainstem water throughout the open water season.

The light energy available at the euphotic surface (PAR curves) show little variation to changes in flow (Figure 6A). This can be explained by the narrow width of the euphotic zone along the shorelines and the constant steep side slopes of the incised channel. The most significant changes in light energy (PAR) are associated with changes in

# FAT CANOE ISLAND (RM 147.1L)

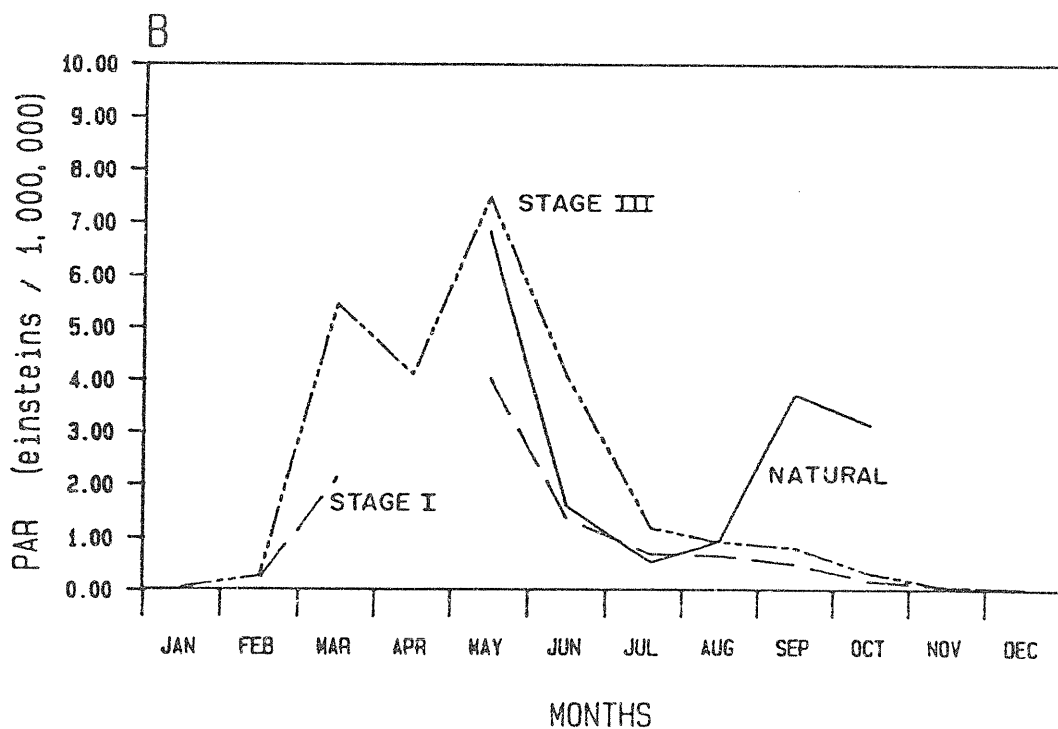
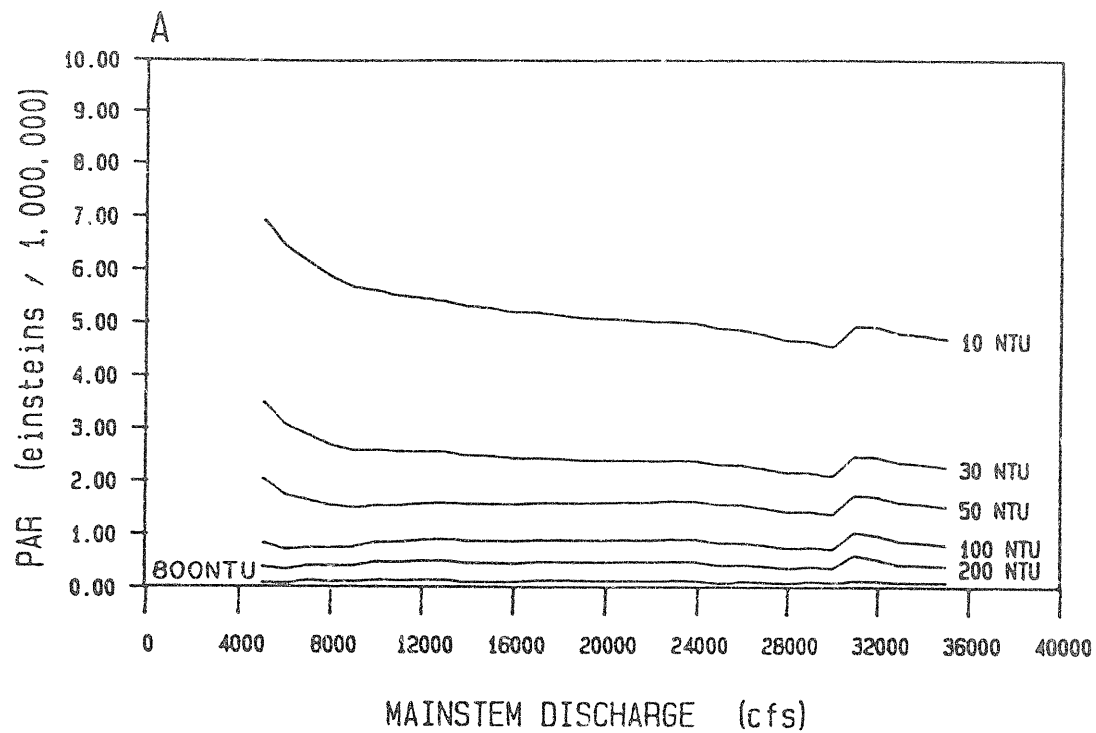


Figure 6. The response of light energy available to the euphotic surface area for (A) turbidity curves and (B) time series curves at Fat Canoe Island

turbidities, which directly affect compensation depth. Between 5,000 cfs and 8,000 cfs, turbidities less than 100 NTU result in descending PAR curves. This is attributable to the slight influence of irregularities in stream profile.

Figure 6B illustrates the time series response of available light energy (PAR) at the Fat Canoe Island site. The most significant difference between natural and with-project trends occurs during late summer and fall (September, October). Energy input to the system during this time is significantly higher under the natural scenario.

#### Whiskers West (RM 101.5L)

This is a large deep side channel similar to that of Fat Canoe Island that also represents mainstem habitat at flows above 10,600 cfs. Below 10,600 cfs this site represents side channel habitat but remains relatively deep. The left bank is steep, and the right bank has a moderate slope. An exposed gravel bar exists at low flows. The study site is approximately 3,200 feet long and 362 feet wide, with a surface area of 27 acres at 23,000 cfs and 21 acres at 10,600 cfs.

The Whiskers West side channel conveys approximately 30 percent of the total mainstem discharge and therefore remains a relatively large channel even at low flows. The PAR response curves, like those illustrated for Fat Canoe Island, are generally insensitive to variations in streamflow (Figure 7A). The anomaly in the PAR response curves between 23,000 and 30,000 cfs reflects the inundation of a shoal

# WISKERS WEST SIDE CHANNEL (RM 101.5L)

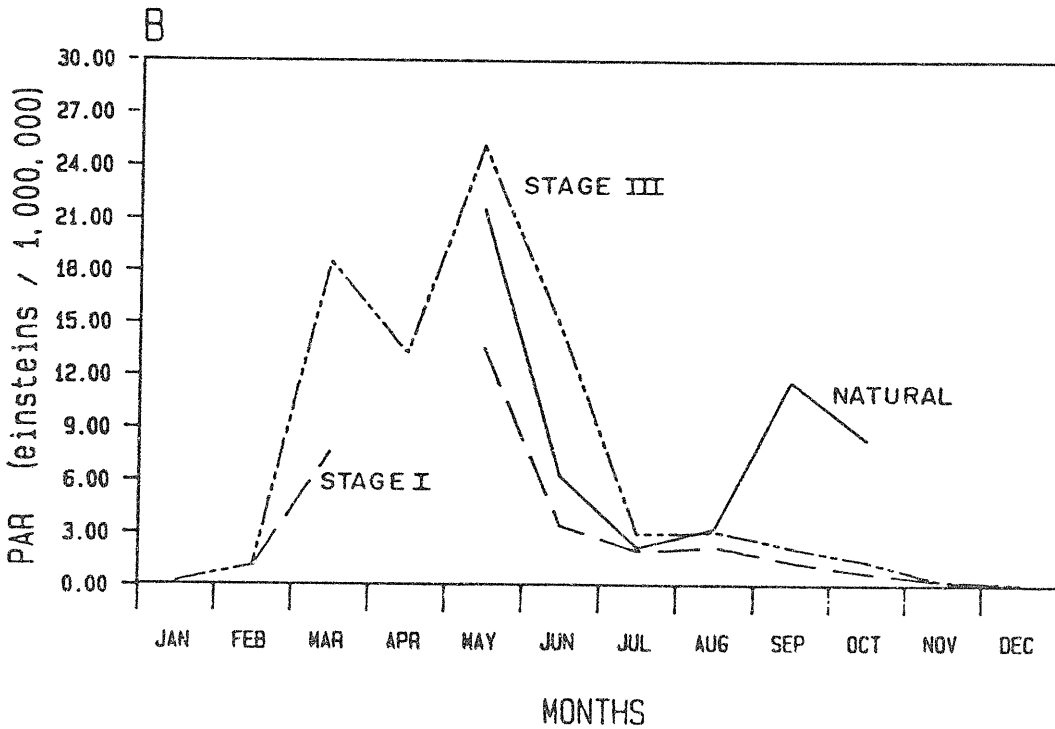
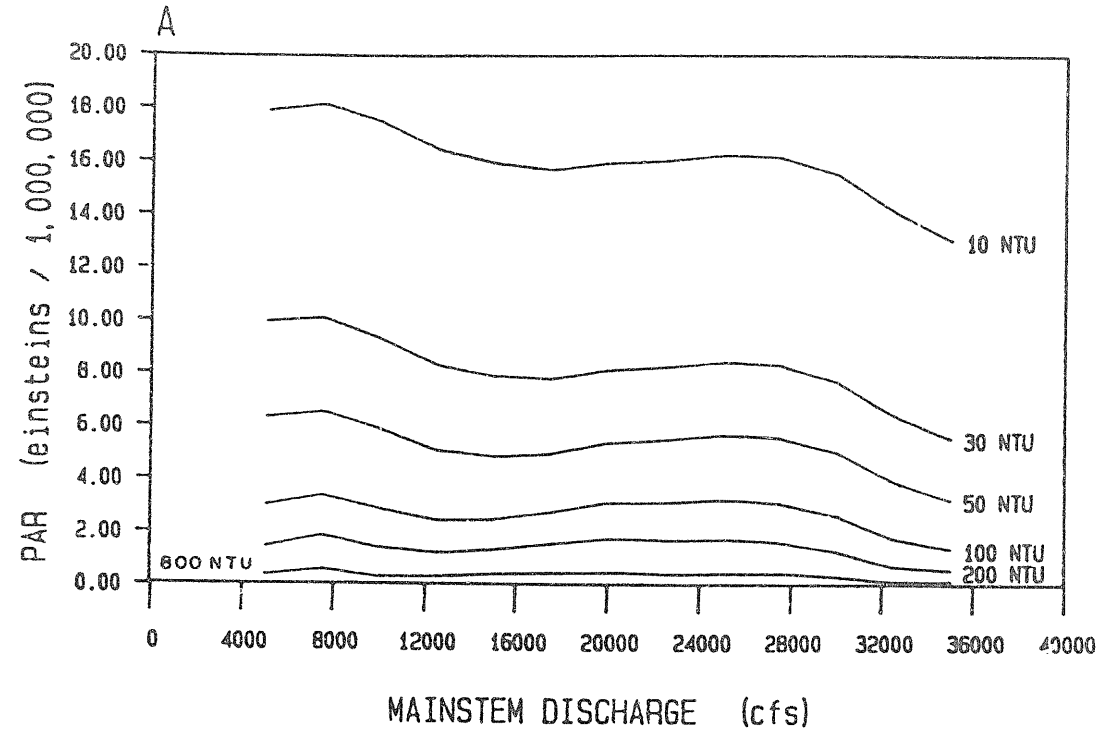


Figure 7. The response of light energy available to the euphotic surface area for (A) turbidity curves and (B) time series curves at Whiskers West Side Channel.

within the upper portion of the model site. As the depth of flow continues to increase over the shoal light intensity decreases. The net effect is reflected in descending PAR curves above 30,000 cfs.

The time series response of PAR at the euphotic surface for Whiskers West (Figure 7B) is similar to that for Fat Canoe Island. A significant difference in available light energy exists between natural and both with-project scenarios during the fall transition period. As both natural and with-project turbidities increase from May to July, all three curves show a significant decrease in available light energy. It is evident that this response is attributable to increasing turbidity, rather than to increasing mainstem discharge because the PAR response curves for all turbidity levels at Whiskers West (Figure 7A) show an insensitivity to variations in mainstem discharge. And like Fat Canoe, Whiskers West shows significantly more light energy available at the euphotic surface in the fall for natural turbidities than for with-project turbidity, even though fall streamflows are similar for all three scenarios.

#### Side Channel 6A (RM 112.6L)

This site and the following site (Fourth of July) are associated with Representative Group VI (refer to Table 4). Side Channel 6A is approximately one mile long and 300 feet wide. At high flows, it typifies mainstem habitat. Between 12,500 and 10,600 cfs, the channel narrows considerably and transforms into riffle/pool habitat found in many large side channels at low flows. The site breaches at a mainstem

discharge less than 5,100 cfs, and thus, conveys turbid water throughout the open water season. The lower half of the site is characterized by extensive mid-channel gravel bars and riffle areas. The upper portion of the study site is characterized by a well defined single channel, both banks of which gradually slope inward to form a broad, parabolic channel. A large gravel bar extends about 1,200 feet downstream from the upstream berm along the left bank. This gravel bar becomes partially exposed and forms a riffle area at mainstem discharges of 11,000 cfs.

Figure 8A shows that the light energy received by the euphotic surface area is influenced by both discharge and turbidity. The interaction of channel geometry and flow has its greatest influence at flows around 8,000 cfs for turbidities less than 50 NTU. At flows greater than about 9,000 cfs, the PAR curves for all turbidity levels descend due to the influence that increased depths have on the total PAR input to the euphotic zone.

The most obvious trend depicted by the time series PAR response curves (Figure 8B) is the increased light energy available to the euphotic surface during the fall transition period under natural conditions, which is suppressed by with-project turbidities. During the summer months (June and July) the available light energy is lower for natural conditions than for with-project conditions. This is attributable to with-project streamflows being less than natural streamflows during this time period, and the influence of mainstem discharge and channel geometry on the energy input to the euphotic surface.

# SIDE CHANNEL 6A (RM 112.61)

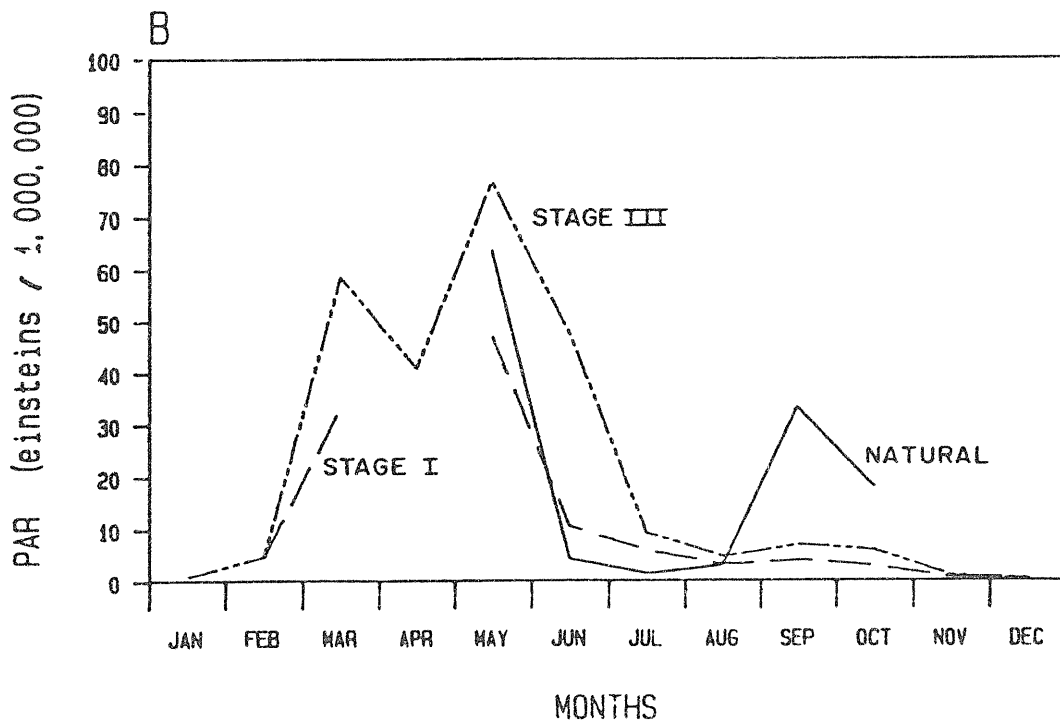
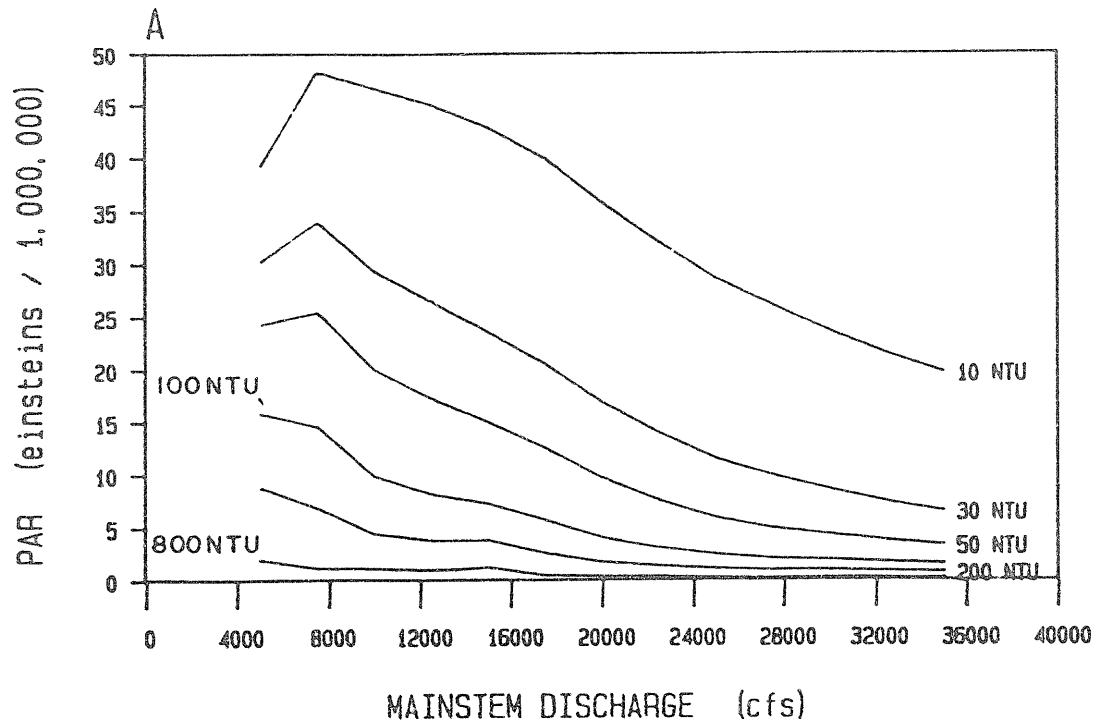


Figure 8. The response of light energy available to the euphotic surface area for (A) turbidity curves and (B) time series curves at Side Channel 6A.

This large side channel represents side channel and mainstem shoal habitat at high flows that transforms to well-defined, single-thread side channel habitat as streamflow decreases. Like Side Channel 6A, this site is associated with Representative Group IV (Table 4). A pool/riffle sequence predominates throughout most of the site at moderate flows. In general, the right bank is gently sloping as compared to the left bank which is moderate to steep. A large, moderate sloping point bar extends from the inside of the bend on the right bank midway through the site. At mainstem flows above 10,000 cfs this bar and the wide shallow channel at the upstream end of the site create extensive shoal areas. The downstream portion of the site is a large, moderately deep backwater zone within a well-defined single channel with steeper banks. Since the breaching flow for this site is about 5,000 cfs, the site generally conveys turbid water throughout most of the open water season.

Figure 9A provides a good illustration of the response of PAR to mainstem discharge and turbidity levels within shoal and riffle areas typically associated with the mainstem and many large side channels. As streamflows rise above 5,000 or 6,000 cfs, water flows out of the thalweg and begins to inundate adjacent gravel bars and mild sloping shoreline areas. As a result, the euphotic surface area increases and available PAR at the streambed increases until depth of flow begins to exceed compensation depth. The PAR curves in Figure 9A show an increase

# FOURTH OF JULY SIDE CHANNEL (RM131.7L)

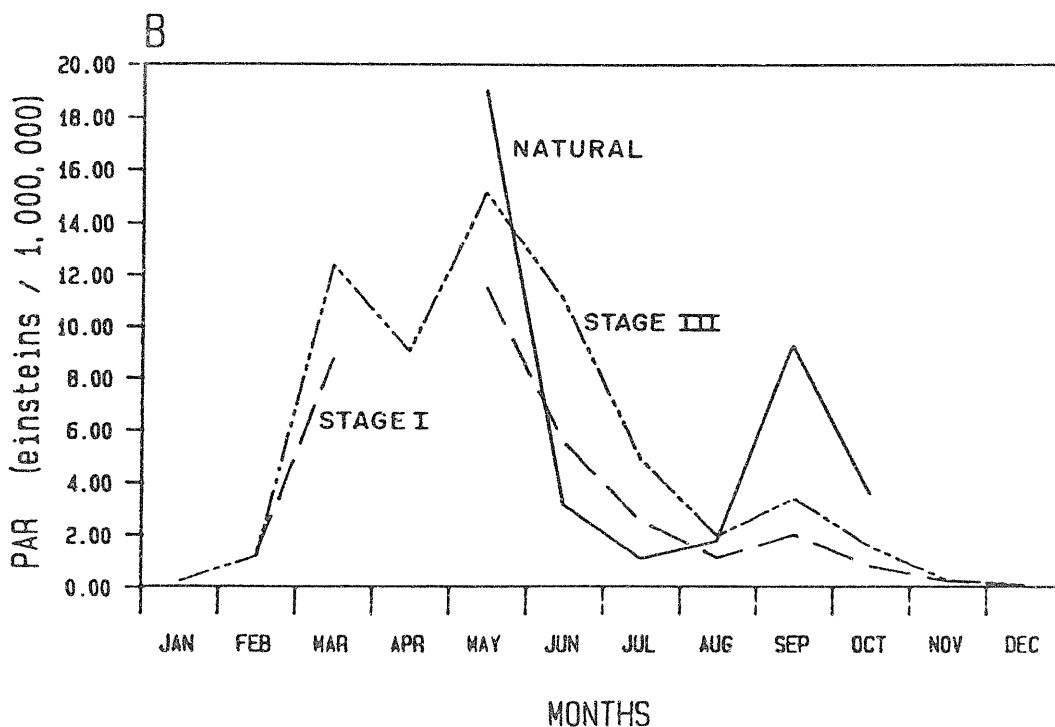
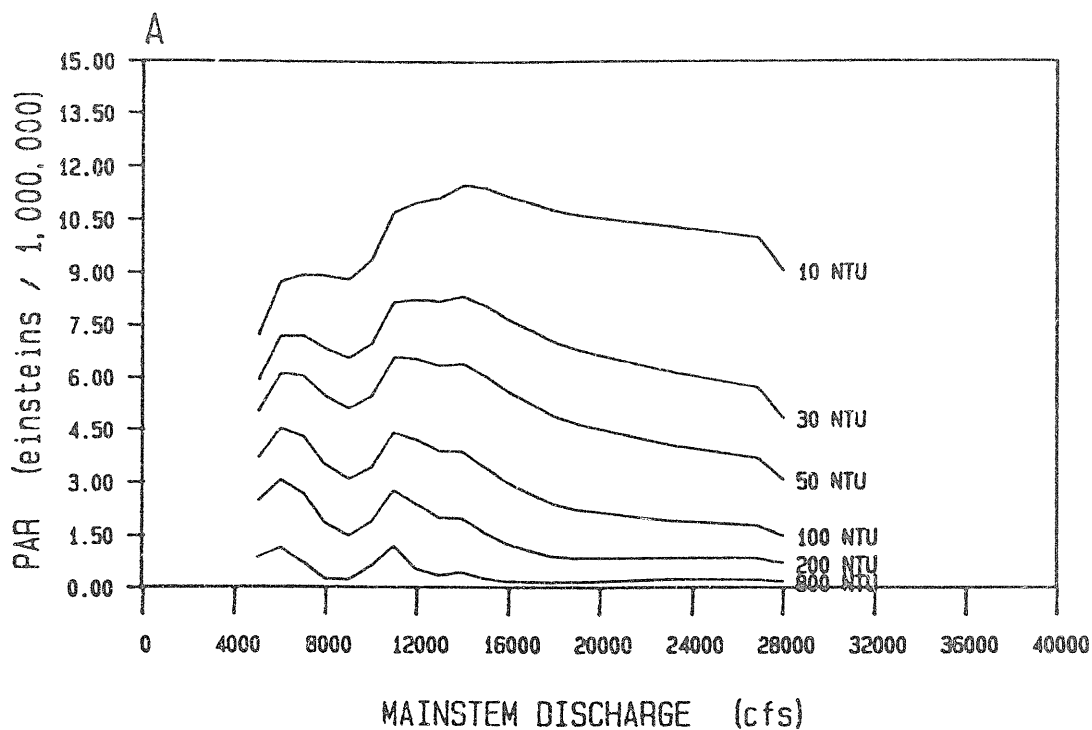


Figure 9. The response of light energy available to the euphotic surface area for (A) turbidity curves and (B) time series curves at Fourth of July Side Channel

and 12,000 cfs. Above this discharge range, the PAR curves decrease for all turbidities greater than 30 NTU.

Review of the time series PAR plots (Figure 9B) indicates that the net effect of forecasted with-project streamflows and turbidities is an increase of available light energy from June through mid-August, but a decrease during fall. This is attributable to the larger amount of shoal area coming into the euphotic zone as a result of lower summer streamflows than occur naturally. Higher than natural fall turbidities and approximately the same streamflows result in a net loss of euphotic area from mid-August through mid-October.

#### Little Rock (RM 119.2R)

This study site represents short, well-defined straight side channels, and is associated with Representative Group VII. It is similar in plan form to many sites in the middle Susitna River. Its channel geometry consists of shallow riffles and gently sloping stream banks in the upstream portion of the site, which gradually transforms into a deep backwater area at the downstream end. This site breaches at a mainstem flow of 10,000 cfs. The wide riffle area at the head narrows considerably at flows below 16,000 cfs. At high flows the riffle disappears and the site becomes a large run and backwater area.

Prior to its head berm being overtopped at mainstem flow of 10,000 cfs, the large backwater area has a significant effect on available light energy. As water surface elevations increase between 5,000 and 7,000 cfs, extension of the water surface further upstream into the site increases the size of the euphotic surface area and the associated energy input to the site. This is reflected by the ascending PAR response for this flow range (Figure 10A). When the head berm is overtopped at 10,000 cfs, there is a substantial increase in wetted surface area (euphotic area). The maximum energy input to the site occurs near 12,000 cfs. Above this flow level, increasing depth and decreasing euphotic surface area causes a gradual decline in the amount of light energy reaching the streambed.

Time series response curves for Little Rock (Figure 10B) reflect trends similar to those described for Fat Canoe Island and Whiskers West. A significant difference in available light energy (PAR) exists between natural and with-project scenarios during the fall. Since fall streamflows are similar and the site is breached for natural and with-project scenarios, the decrease in PAR values at the streambed are principally a function of higher with-project turbidities.

#### Upper Side Channel 11 (RM 136.3R)

This site is similar to Little Rock except that its head berm is not breached until 13,000 cfs, and mainstem discharge does not have a pronounced effect on the site until about 16,000 cfs. Prior to breaching, streamflow in the channel is maintained by groundwater inflow. A backwater also exists at the mouth of this site at moderate

# LITTLE ROCK (RM 119.2R)

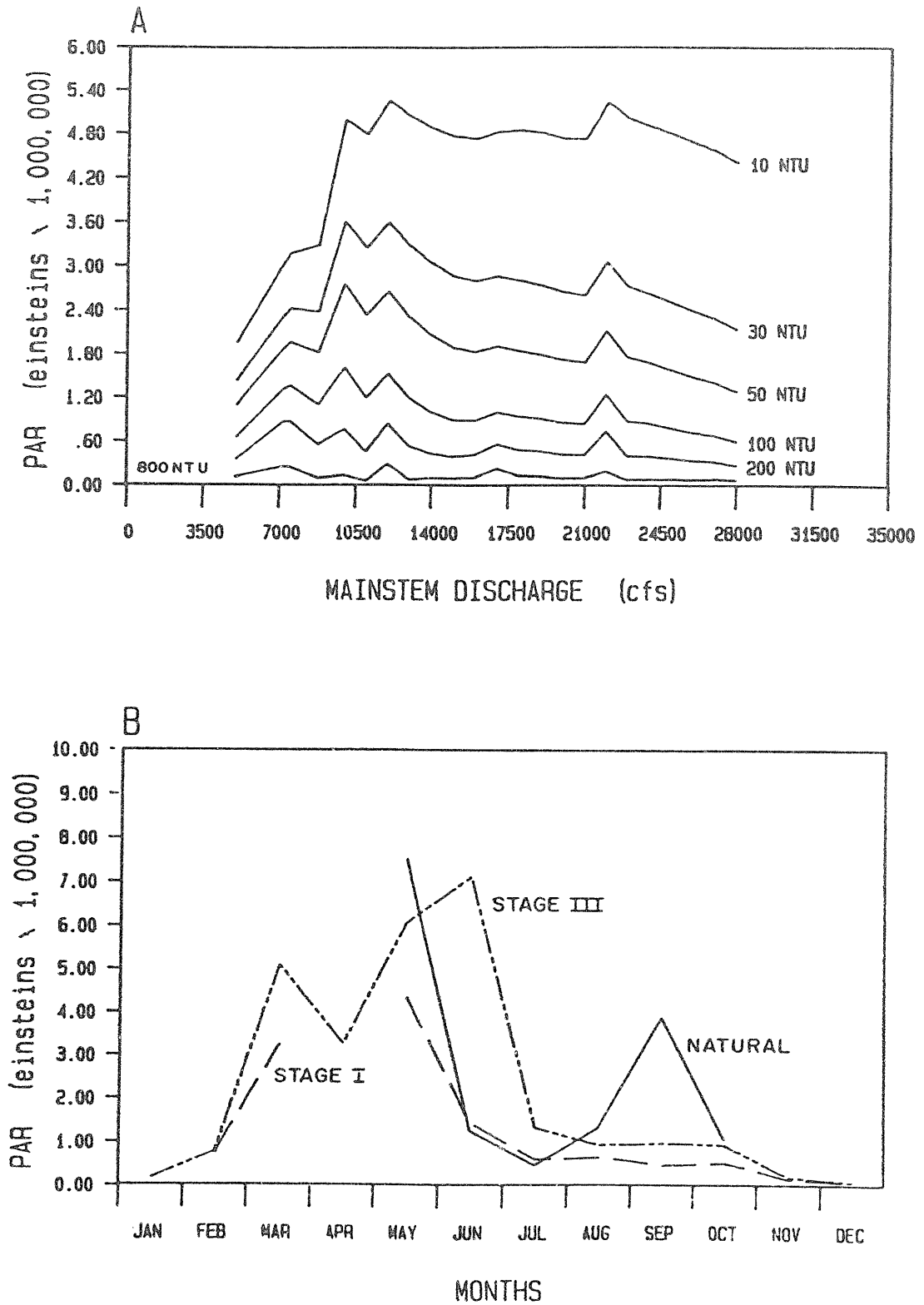


Figure 10. The response of light energy available to the euphotic surface area for (A) turbidity curves and (B) time series curves at Little Rock site.

mainstem discharge. The area upstream from the backwater is dominated by a long, shallow riffle that transforms into a moderately deep run as mainstem discharge increases. Both the right and left streambanks possess exposed shorelines of moderate slope except when inundated by high streamflows.

The available light energy at this site responds differently to the influence of mainstem discharge above 16,000 cfs depending upon turbidity (Figure 11A). When the site is controlled by mainstem discharge above 16,000 cfs, the available light energy decreases if turbidities are greater than 50 NTU. Below 50 NTU, the influence of controlling mainstem flow increases PAR values. The apexes of the PAR curves for turbidities less than 50 NTU are found around 28,000 cfs, while for higher turbidities, the maximum energy input occurs around 16,000 cfs.

The time series response curves (Figure 11B) indicate with-project streamflows and turbidities would increase PAR at the streambed throughout summer. During the fall, a small decrease would exist. This is attributable to the backwater and unbreached conditions existing for both scenarios and the relatively shallow depths in the site under these conditions.

#### Slough 9 (RM 128.8R)

This site is typical of long sinuous sloughs that are breached at intermediate mainstem discharges (16,000 cfs). Slough 9 is associated with Representative Group II. Below 16,000 cfs the site transforms from

# UPPER SIDE CHANNEL 11 (RM 136.3R)

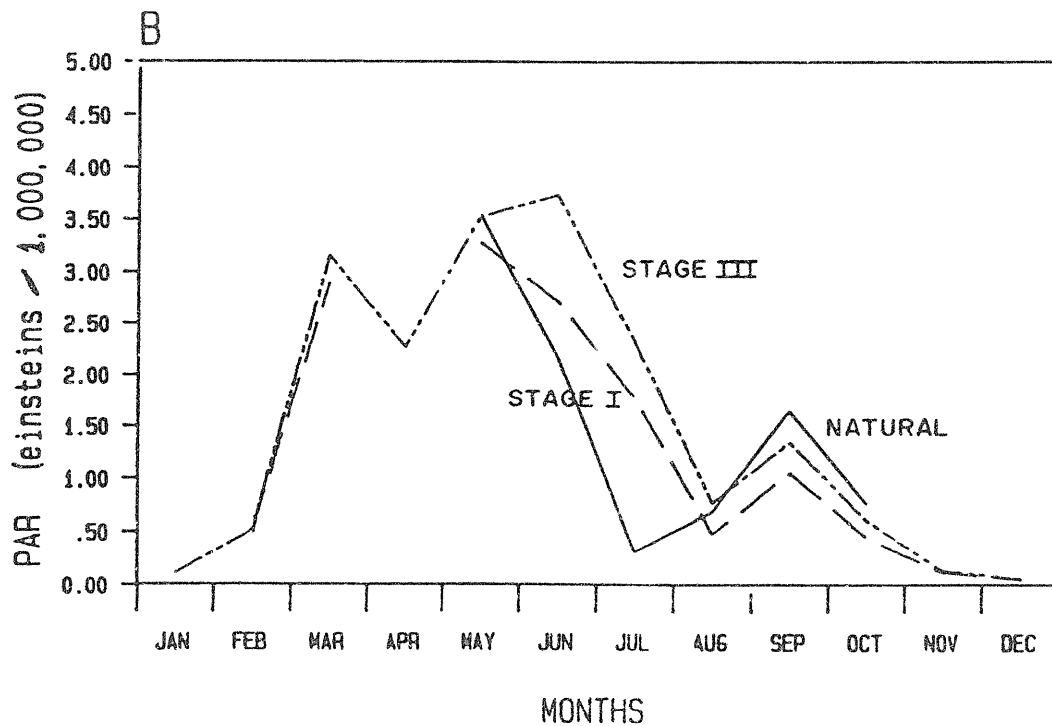
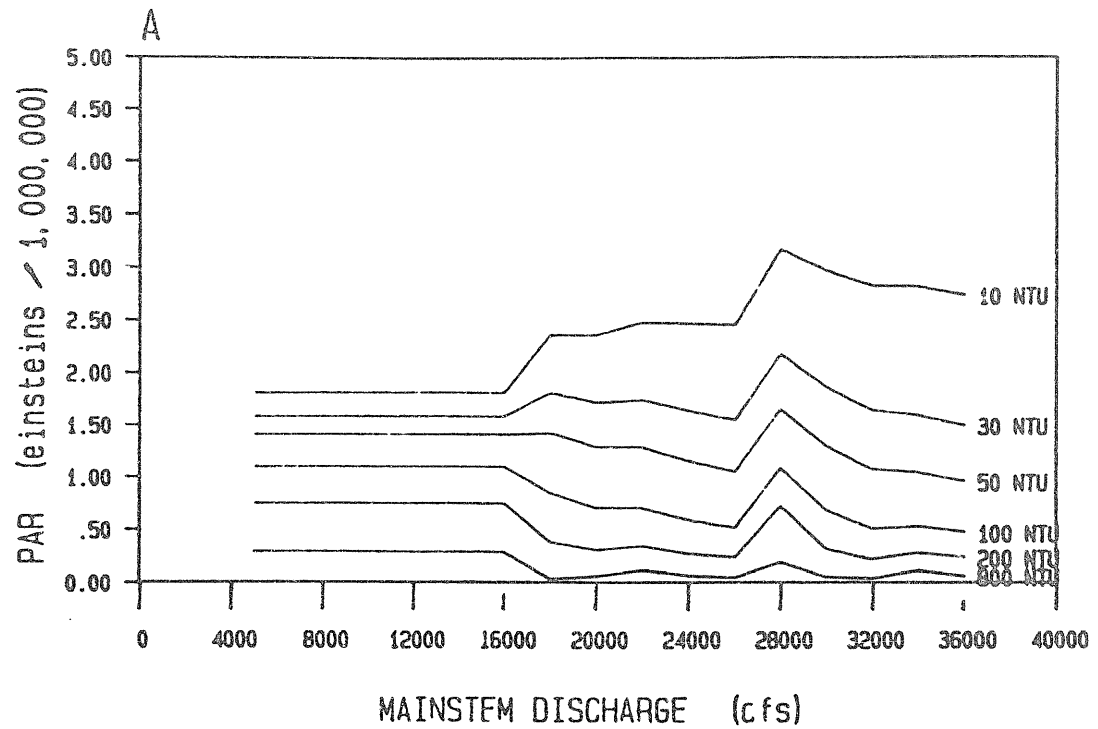


Figure 11. The response of light energy available to the euphotic surface area for (A) turbidity curves and (B) time series curves at Upper Side Channel 11.

a turbid side channel to a clearwater slough maintained by small tributaries and groundwater. The upper portion of the study site consists of pool habitat with a vertical right bank and a mild sloping left bank. The middle portion of the site is principally riffle and run habitat with both banks having a mild slope. At high flows, the entire site becomes a long run with a backwater area at its downstream end.

The PAR response curves for Slough 9 reflect a sharp increase in the available light energy above 16,000 cfs (Figure 12A). This is a result of the head berm being overtopped and dramatic increase in wetted surface area. Although clearwater exists at this site below a mainstem discharge of 16,000 cfs, the wetted surface area is too small to influence the responses of the PAR curves.

The time series PAR response curves for Slough 9 converge to form one line for the fall transition period (September and October) (Figure 12B). This occurs because both natural and with-project fall streamflows are insufficient to breach the site and clearwater flow exists under both scenarios. During summer, with-project flows are also insufficient to overtop this site and slough flow remains clear. Hence, substantially more PAR is available at this site throughout the year for both with-project scenarios than occurs naturally.

# SLOUGH 9 (RM 128.8R)

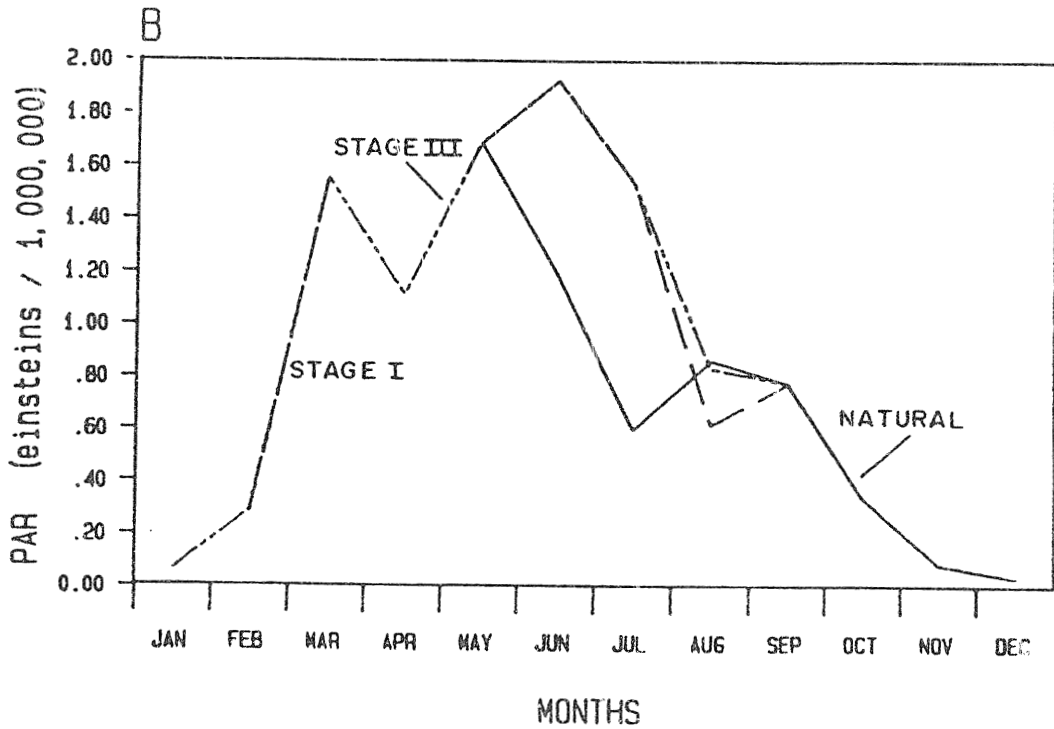
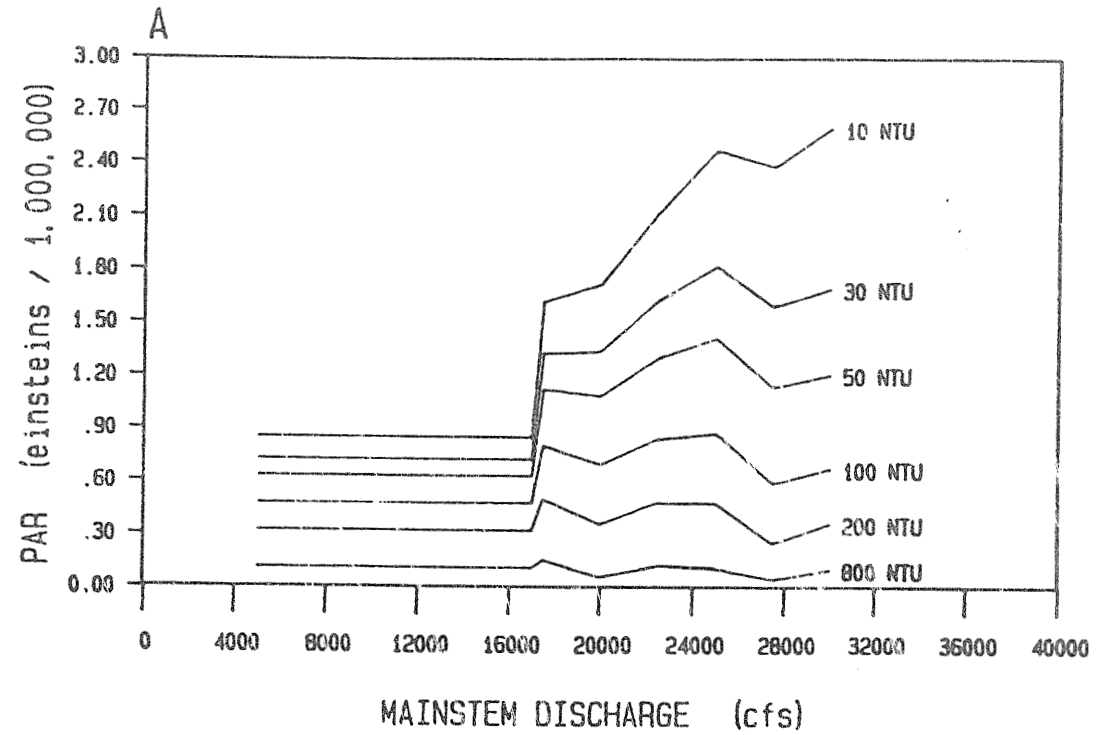


Figure 12. The response of light energy available to the euphotic surface area for (A) turbidity curves and (B) time series curves at Slough 9.

### Slough 8A (RM 126.0R)

This site is typical of side sloughs that are breached at very high mainstem discharges (33,000 cfs). This site is in Representative Group II. The site is approximately two miles in length with an average width of about 100 feet. It is separated from the mainstem by two large vegetated islands. Both the right and left banks are relatively steep and similar to those found in tributary streams. Below the breaching discharge of 33,000 cfs, approximately 10 cfs of clearwater flow is provided by local runoff and groundwater.

The PAR response functions for Slough 8A are similar to those for Slough 9. Below the breaching flow, the PAR response curves do not respond to mainstem discharge (Figure 13A). Above 33,000 cfs the curves descend abruptly as a result of turbid mainstem water entering the site. This is opposite to that trend evident at Slough 9 (Figure 12A). The trend at Slough 8A is attributable to mainstem flow being contained within the steep banks of the channel allowing an insignificant increase in wetted surface area while the increase in depth decreases available light energy at the streambed.

The time series response curves for Slough 8A are shown in Figure 13B. These response curves reflect the influence of the high breaching flow (33,000) at this site in comparison to the average monthly mainstem discharges for natural and with-project conditions that do not exceed 33,000 cfs. Hence, site-specific flow and turbidity values are the same

# SLOUGH 8A (RM126.0R)

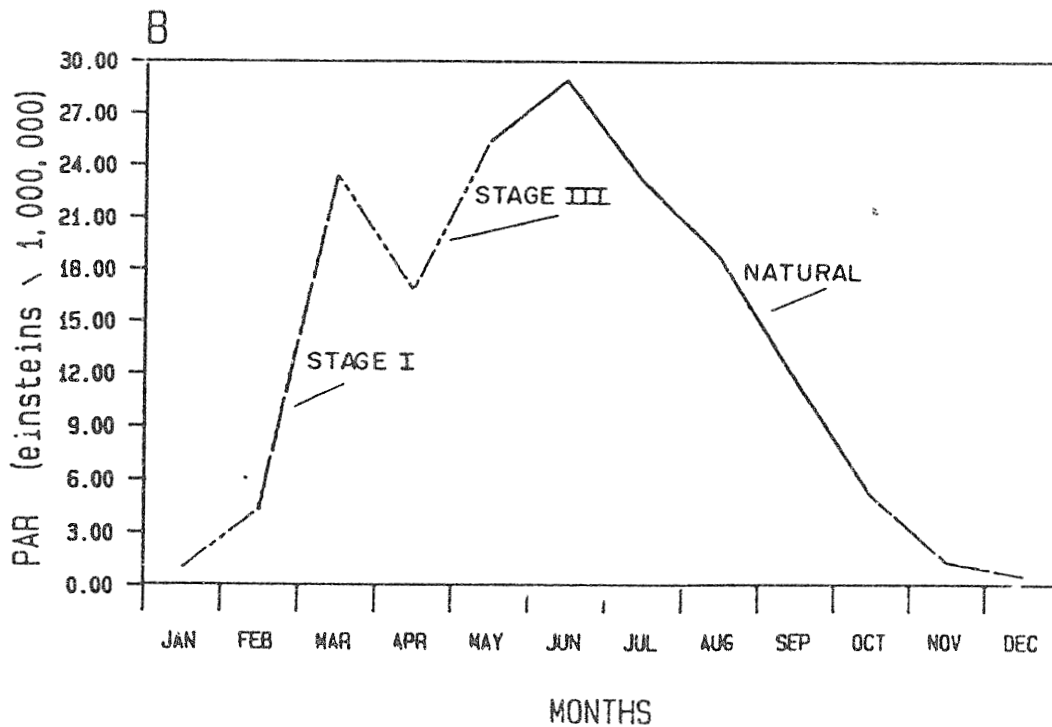
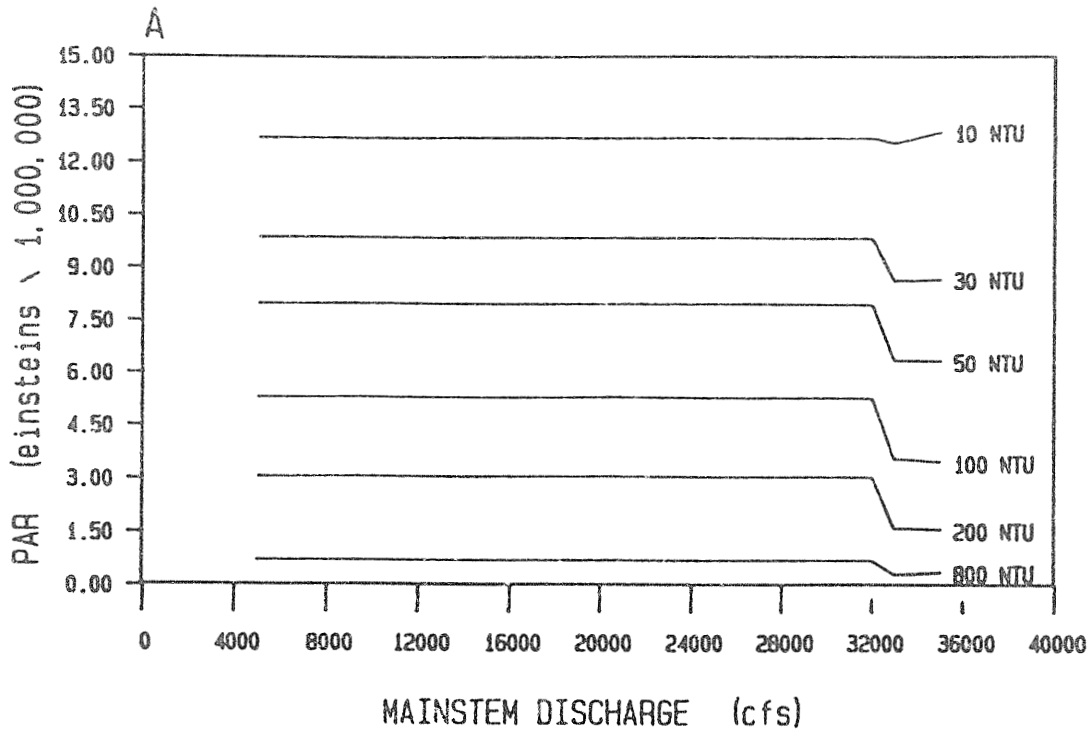


Figure 13. The response of light energy available to the euphotic surface area for (A) turbidity curves and (B) time series curves at Slough 8A

for all three scenarios, and the single time series PAR curve represents both natural and with-project conditions. The shape of the curve reflects only the seasonal change in solar radiation.

## SUMMARY

A model was developed that estimates the amount of photosynthetically active radiation (PAR) available to the euphotic zone at selected sites in the middle Susitna River. The model was designed to accept four input variables: (1) mainstem discharge, (2) turbidity, (3) solar insolation, and (4) channel geometry. Channel geometry varies according to the site selected. The remaining three variables are seasonally dependent, but natural variation in mainstem discharges and turbidity will be affected by project development. The purpose of the model was to estimate the effects of altered mainstem discharge and turbidity regimes on PAR.

The model was developed in three general steps. The first step simply estimated the amounts of euphotic surface area available at each site under different combinations of mainstem discharge and turbidity. This provided insight into how available surface area responds to alterations in these two variables. The second step included a constant solar input and the attenuation of this energy with depth under the same mainstem discharge and turbidity regimes analyzed in step 1. The results of step 2 provided an analysis of photosynthetically usable light energy from a constant solar input reaching the surface areas calculated in step one and the effects of mainstem discharge and turbidity on that energy. Finally, step 3 correlated turbidity with mainstem discharge as they covary in the middle Susitna River naturally, and as they are expected to covary under with-project conditions. Monthly combinations of turbidity and mainstem discharge were then used in the model in a time-series incorporating monthly variations in solar insolation. The end

results were estimates for the amount of PAR reaching the euphotic surface areas at each site during the course of a year for both with-project and natural conditions. Three conclusions can be drawn from the results:

First, photosynthetically available light energy is universally sensitive to changes in turbidity. That is, at all sites, the total amount of light energy that reaches the euphotic zone increases as turbidity declines. Although this should be intuitively obvious, it must be included in a discussion of conclusions because of its extreme importance.

Second, mainstem discharge significantly influences light input to the euphotic zone only at selected sites, those with large shoal and riffle areas, such as Fourth of July and Side Channel 6A, and those that are likely to be influenced by the effects of breaching flows, such as Upper Side Channel 11 and Slough 9. These sites exhibit optimal energy input to the euphotic zone at specific mainstem discharges.

Third, the model illustrates that whether the project will have positive, neutral, or negative effects on the amount of PAR reaching submerged surfaces depends upon the specific site affected, the time of the year, and the operational flow regimes selected. By applying those flow regimes selected under the Case E-VI scenario to the model, two further conclusions are supported:

(1) Given the estimated with-project turbidities presented in the License Amendment, the project will have significant negative effects on the amount of PAR available to the euphotic zone only in the fall, and then, only at selected sites. Those sites that will be affected are those that have low breaching flows, relatively deep channels, and are associated with mainstem or side channel habitat. Examples are Fat Canoe, Whiskers West, Side Channel 6A, Little Rock, and Fourth of July Side Channel. The predicted reductions in PAR at these sites under with-project conditions are a result of their relatively low breaching flows. Thus, regardless of whether the project is constructed, these sites will convey water all year. But under with-project conditions, negative impacts on PAR will occur because of increased turbidities in the fall. Other sites (e.g., Upper Side Channel 11) with intermediate breaching flows may also be affected, but not as greatly because of the influence of turbidity inflow and upwelling in maintaining clearwater input to these sites.

(2) Beneficial effects from the project may occur during the summer months at almost all sites for two reasons: (1) the reduction of turbidities expected during these months, and (2) the effect of lower flows and water surface elevations exposing more of the bottom to PAR. Again, however, these conclusions are supported only by the turbidity regimes presented in the amendment. The most pronounced increases in euphotic energy input under with-project conditions will occur at those sites that demonstrate optimal amounts of euphotic surface areas at flows that correspond to with-project flows during the summer.

## REFERENCES

- Aaserude, R.G., J. Thiele, and D. Trudgen. 1985. Categorization and characterization of aquatic habitat types of the middle Susitna River. E. Woody Trihey and Associates, Anchorage, AK. Technical memorandum. 1 vol.
- Acres American Inc. 1982. Feasibility report. Volume 2. Environmental report. Sections 104. Final draft, Alaska Power Authority. Susitna Hydroelectric Project. 1 vol.
- Alaska Dept. of Fish and Game, Susitna Hydro Aquatic Studies. 1982. Phase I final draft report. Aquatic studies program. Report for Acres American Inc. Alaska Power Authority. Susitna Hydroelectric Project. 1 vol.
- Alaska Dept of Fish and Game, Susitna Hydro Aquatic Studies. 1983a. Phase II basic data report. Vol. 4: Aquatic habitat and instream flow studies, 1982. Anchorage, AK. Part 1, p. 2.
- Alaska Dept. of Fish and Game, Susitna Hydro Aquatic Studies. 1983b. Phase II basic data report. Vol. 4: Aquatic habitat and instream flow studies, 1982, appendices D-J. 1 vol.
- Alaska Power Authority. 1985. Before the Federal Energy Regulatory Commission. Application for license for major project. Susitna Hydroelectric Project draft license application. Prepared by Harza-Ebasco Susitna Joint Venture. Susitna Hydroelectric Project. 17 vols.
- Branton, C.I., R.H. Shaw, and L.D. Allen. 1972. Solar and net radiation at Palmer, Alaska 1960-71. University of Alaska Institute of Agricultural Sciences Technical Bulletin, Number 3. 8 pp.
- Chow, V.T., ed. 1964. Pages 10-29 In Handbook of applied hydrology, an compendium of water-resources technology. McGraw-Hill, NY.
- Coffin, J.F. 1984. Solar and longwave radiation data for Southcentral Alaska. In: Alaska's water: A critical resource (S.R. Bredthauer, chairman). Proceedings Alaska Section American Water Resources Association. Institute of Water Resources. University of Alaska-Fairbanks. Report IWR-106.
- Estes, C.C., and D.S. Vincent-Lang, eds. 1984. Report No. 3. Aquatic habitat and instream flow investigations (May-October 1983). Chapter 4: Water quality investigations. Susitna Hydro Aquatic Studies, Alaska Dept. of Fish and Game. Report for Alaska Power Authority, Anchorage, AK. Document 1933. 1 vol.

- E. Woody Trihey and Associates and Woodward-Clyde Consultants. 1985. Working draft. Instream flow relationships report. Volume No. 1. Alaska Power Authority, Susitna Hydroelectric Project Report for Harza-Ebasco Susitna Joint Venture. Anchorage. AK.
- Hilliard, N.D., et al. 1985. Hydraulic relationships and model calibration procedures at 1984 study sites in the Talkeetna-to-Devil Canyon segment of the Susitna River, Alaska. E. Woody Trihey and Associates. Report for Alaska Power Authority, Anchorage, AK. 1 vol.
- Hynes, H.B.N. 1979. The ecology of running waters. University of Toronto Press. 555 pp.
- James, H.R., and E.A. Birge. 1938. A laboratory study of the absorption of light by lake waters. Trans. Wis. Acad. Sci. Arts Lett. 31:1-154. 381-383.
- Lloyd, D.S. 1985. Turbidity in freshwater habitats in Alaska. Habitat Div., Alaska Dept. of Fish and Game. Juneau, AK. 101 pp.
- Milhous, R.T., D.L. Weyner, and T. Waddle. 1984. Users guide to the Physical Habitat Simulation System. Instream Flow Information Paper 11. U.S. Fish Wildl. Serv. FWS/OBS - 81/43 revised. 475 pp.
- Moss, B. 1980. Ecology of fresh waters. John Wiley and Sons, NY. 332 pp.
- Ott Water Engineers Inc. 1981. Bradley Lake Water Quality Report. Prepared for U.S. Army Corps of Engineers, Alaska District, Anchorage, AK. September, 1981.
- Reub, G.R., E.W. Trihey, and C. Wilkinson. 1985. Preliminary analysis of the influence of altered middle river discharge and turbidity regimes on the surface area of the euphotic zone. E. Woody Trihey and Associates, Anchorage, AK. Technical memorandum. 25 pp.
- R&M Consultants. 1982. Glacial Lake Studies. Prepared for Acres American Inc.
- Roulet, N.T. and W.P. Adams. 1984. Illustration of the spatial variability of light entering a lake using an empirical model. Hydrobiologia 109:67-74.
- Rowe, T.G. 1985. Seasonal variation of photosynthetically active radiation in Big Lake, southcentral Alaska. In: Resolving Alaska's water resource conflicts (Linda Perry Dwight, chairman). Proceedings Alaska Section American Water Resources Association. Institute of Water Resources. University of Alaska-Fairbanks. Report IWR-108. 212 pp.
- Scott, K.M. 1982. Erosion and Sedimentation in the Kenai River, Alaska. USGS Professional Paper No. 1235. 35 pp.

Van Nieuwenhuyse, E.E. 1983. The effects of placer mining on the primary productivity of Interior Alaska streams. M.S. Thesis, University of Alaska-Fairbanks. 120 pp.

Van Nieuwenhuyse, E.E. 1984. Preliminary analysis of the relationships between turbidity and light penetration in the Susitna River, Alaska. E. Woody Trihey and Associates, Anchorage, AK. Technical memorandum. 7 pp.